Cavity QED with Single Atoms and Photons

T. E. Northup, K. M. Birnbaum, A. Boca, A. D. Boozer, J. McKeever, R. Miller, and H. J. Kimble

Norman Bridge Laboratory of Physics 12-33, California Institute of Technology, Pasadena, CA 91125

Abstract. Recent experimental advances in the field of cavity quantum electrodynamics (QED) have opened new possibilities for control of atom-photon interactions. A laser with "one and the same atom" demonstrates the theory of laser operation pressed to its conceptual limit [1]. The generation of single photons on demand and the realization of cavity QED with well defined atomic numbers $N = 0, 1, 2, \ldots$ both represent important steps toward realizing diverse protocols in quantum information science [2, 3]. Coherent manipulation of the atomic state via Raman transitions provides a new tool in cavity QED for *in situ* monitoring and control of the atom-cavity system. All of these achievements share a common point of departure: the regime of strong coupling. It is thus interesting to consider briefly the history of the strong coupling criterion in cavity QED and to trace out the path that research has taken in the pursuit of this goal.

Keywords: quantum optics, particle traps, Raman spectra
PACS: 42.50.Vk, 42.50.Ct, 32.80.Pj

RATES AND RATIOS OF CAVITY QED

In 1946, E. M. Purcell [4] pointed out the dependence of the Einstein-A coefficient on boundary conditions. Subsequent theoretical work [5, 6] showed that the probability of spontaneous emission could be characterized by a parameter β:

$$\beta \sim A\{(1-\frac{\Delta\Omega}{4\pi})+(boundary\,function)\times\frac{\Delta\Omega}{4\pi}\} \quad (1)$$

where $\Delta\Omega$ is the solid angle associated with the atom-boundary interaction. Note that the first term leads to an inhibition (reduction) in the rate β below A. However, the magnitude of the boundary function in the second term determines whether the overall rate β will be greater or less than the rate of free space decay. A separate effect of the boundary is to induce shifts in the atom's energy levels, which in general vary with position near the boundary and hence lead to forces on an atom. More specifically, an atom in the excited state experiences a London-van der Waals force due to an induced dipole, while for a ground state atom, spatial variations of the Lamb shift generate a Casimir-Polder force [6, 7, 8]. These frequency shifts are significant enough to be experimentally observable [9], and are extremely important for precision measurement of the electron g factor for one electron in a Penning trap [10, 11, 12].

Thus we see that the presence of boundaries results in an interaction with an altered structure of modes for the electromagnetic field to which a quantum radiator can transfer energy. In general, atomic decay arises from excitation incoherently lost to a continuum of modes. However, for the idealized boundary condition of a lossless optical resonator

CP770, *Atomic Physics 19,* edited by L. G. Marcassa, K. Helmerson, and V. S. Bagnato

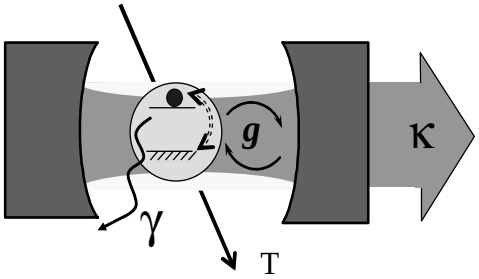

FIGURE 1. Characteristic parameters of atom, cavity, and environment: κ, the rate of decay of the cavity field; γ, the rate at which the atomic dipole radiates into modes other than the cavity field mode; T, the transit time of an atom through the cavity mode; and g, the rate of coherent atom-field coupling. Strong coupling requires that $g/(\gamma, \kappa, \frac{1}{T}) \gg 1$.

(cavity), an atom interacts with a localized, single mode, which can then return the energy to the atom. The result is a coherent transfer of quanta between atom and radiation field, described in the seminal paper of Jaynes and Cummings in 1963 [13]. In this idealized setting, the Hamiltonian of the atom-cavity system is given by [14, 15]

$$H = \hbar\omega_{cavity} a^{\dagger} a + \hbar\omega_{atom} \frac{\sigma_z}{2} + \hbar g(a^{\dagger}\sigma_{-} + \sigma_{+} a), \tag{2}$$

where ω_{cavity} is the resonant frequency of the cavity and ω_{atom} is the frequency spacing the between the atom's ground and excited states. Single-photon Rabi nutation between the atom and cavity occurs at a frequency $2g$. The Rabi frequency is proportional to the electric field per photon, namely

$$g \equiv \frac{\mu}{\hbar}\sqrt{\frac{\hbar\omega_{cavity}}{2\varepsilon_0 V_{mode}}}, \tag{3}$$

where μ is the atomic dipole moment and V_{mode} is the cavity mode volume. Note that a small mode volume is thus essential to achieve a large Rabi frequency for single photons.

Of course, a physical cavity is not lossless; photons leave at a rate 2κ which is proportional to the cavity's quality factor. Additionally, the atomic excited state population decays at rate $2\gamma \approx A$, which is close to the free-space atomic decay rate because of the small solid angle subtended by optical cavities relevant to our work. A third parameter of the cavity QED system is the time T during which the atom interacts with the cavity mode. In the language of open quantum systems, κ, γ, and $\frac{1}{T}$ characterize rates of irreversible decay to the environment, while g is the rate of coherent evolution of the system. In order for the atom and cavity to exchange quanta of energy over many cycles, we require that [14]

$$g/(\gamma, \kappa, \frac{1}{T}) \gg 1 \tag{4}$$

This is the strong coupling criterion.

Strong coupling permits us to define two figures of merit: the critical photon number $m_0 \equiv \frac{\beta^2}{2g^2}$ and the critical atom number $N_0 \equiv \frac{2\beta\kappa}{g^2}$, where $\beta \equiv max[\gamma, \frac{1}{T}]$. When the critical

photon number is less than one, nonlinear optics with one photon per mode becomes possible. When the critical atom number is less than one, only a single atom is required for appreciable modifications of the response of an optical cavity (e.g., switching).

EXPERIMENTS IN THE STRONG COUPLING REGIME

State-of-the-art experiments in cavity QED in the optical domain have achieved typical values of $m_0 \sim 10^{-3}$ to 10^{-4} photons and $N_0 \sim 10^{-2}$ to 10^{-3} atoms. One important step in reaching such low values has been the use of superpolished mirrors with multilayer dielectric coatings; optical resonators built with these mirrors have very low losses and thus a low κ, while placing the mirrors tens of microns apart insures a small V_{mode} and thus a large g. But in achieving long cavity times T which minimize β, it was the merger of laser cooling and trapping techniques with the cavity QED environment [16] which proved a significant breakthrough. The first demonstrations of the strong coupling criterion with atoms in optical resonators [17, 18] had relied on atomic beam transits through the cavity mode; thus, measurement data represented an average over an ensemble of atoms. But by capturing a cloud of cesium atoms in a magneto-optic trap (MOT) millimeters above a cavity, then releasing them at sub-Doppler temperatures to fall between the mirrors, individual atomic trajectories could be witnessed in real time [16].

These early technical achievements have made possible a diverse collection of recent experiments. For example, G. Rempe's group at the Max Planck Institute in Garching has used the atom-cavity coupling as a means to cool the motion of an intracavity atom [19]; the authors estimate that "the observed cooling rate is at least five times larger than that produced by free-space cooling methods, for comparable excitation of the atom." When one applies a blue-detuned probe laser to the cavity, the motion of a trapped atom transfers energy to the cavity field, and this energy subsequently leaves the system through the process of cavity decay.

Another interesting result relates to the propagation of optical pulses through a high finesse atom-cavity system [20]. Previously, pulses with dramatically shifted group velocities have been observed propagating through dense atomic media, which are necessary to generate a steep gradient of the refractive index [21]. But in the work of Shimizu et al. [20], a cavity with $N_0 \ll 1$ allows just a handful of intracavity atoms to substitute for a macroscopic free-space ensemble. While the experimenters have not yet obtained single-atom resolution in their cavity, if such an atom were to be trapped and prepared in a superposition of ground states, it could then map these ground states to two time-separated optical pulses.

Finally, the use of an optical dipole "conveyor belt" to transport single atoms [22] into and out of the cavity interaction region offers new possibilities for control of cavity QED systems and perhaps a means to achieve a scalable architecture for quantum computation. The group of M. Chapman at Georgia Tech has used such a one-dimensional optical lattice to transport Rubidium atoms back and forth through a cavity mode, observing their passage by monitoring transmission of a probe beam at the cavity output [23].

We would also like to highlight exciting recent progress in the ion-trapping community, notably the generation of single photons from a Ca^+ ion in a cavity [24, 25] and the use of a miniature rf-Paul trap to couple an ion to a high finesse cavity mode [26]. While these groups have not yet realized the strong coupling criterion, their precise control of atomic position and their extended trapping times remain unmatched by neutral atom experiments.

STRONG COUPLING AT CALTECH

For our research group, a major advance towards the realization of strong coupling with single trapped atoms occurred in 1996, when we successfully combined the techniques of laser cooling and trapping with those of cavity QED and thus observed the first individual atomic transits through a cavity [16, 14]. Subsequent work pursued the goal of localizing these single atoms in a regime of strong coupling. To this end, a near-resonant probe beam with mean field strength of one photon was used to trap a single atom in a cavity mode for times up to ~ 1 ms [27, 28]. The high rate of optical information carried by the transmitted field, much greater than the possible rate from a free-space atom, allowed real-time reconstruction of individual atomic trajectories.

However, another experiment in our group was actually the first to achieve trapping of single atoms in a regime of strong coupling. Here, we utilized a far off-resonant trap (FORT) to generate a conservative dipole-force potential along a second longitudinal cavity mode [29]. A cloud of cold atoms was released from a MOT, with a few atoms falling between the cavity mirrors and into the cavity mode. The presence of an intracavity atom, sensed in real time with a cavity probe beam, was then used to activate a FORT beam to confine the atom within the cavity. Early difficulties in this experiment were caused by cavity-enhanced FM-to-AM noise conversion that prompted us to search for a new FORT wavelength further detuned from the 852 nm Cesium line, where our cavity has maximal finesse. This in turn led to the implementation of a "magic" FORT wavelength at 936 nm [30, 31, 32]. A FORT will ordinarily generate AC-Stark shifts of opposite signs for the ground and excited states of an atomic transition, but for a FORT at 936 nm in Cesium, both the ground and excited states of the D_2 transition have negative, approximately equal shifts. We thus demonstrated a novel mechanism for state-insensitive trapping, allowing us to decouple the atom's center-of-mass motion from its internal degrees of freedom and to perform transformations via excited atomic states that are largely free of trap-induced heating.

This trapping ability has recently enabled a series of advances in Quantum Optics and Quantum Information Science in our laboratory. We have observed individual Cesium atoms confined within the FORT with lifetime $\tau \simeq 3$ s; even while being continuously monitored via transmission of a strongly coupled probe beam, the atoms remain trapped for $\simeq 1$ second [33]. A single trapped atom can then act as the active medium in a one-atom laser, a new device which exhibits qualitatively different behavior from a conventional laser with many atoms and photons [1]. In this experiment an applied field Ω_3 from the side of the cavity (i.e., transverse to the cavity axis) pumps the atom from ground state $(6S_{1/2}, F = 3)$ to excited state $(6P_{3/2}, F' = 3')$, which strong coupling maps to $(6S_{1/2}, F = 4)$ via emission of a photon into the cavity (lasing) mode; a

second applied field Ω_4 pumps the atom to $(6P_{3/2}, F' = 4')$, from which it spontaneously decays to the original ground state. Conventional laser theory requires critical photon and atom numbers $m_0, N_0 \gg 1$ and thus is not applicable in the strong coupling regime. Experimentally, we observe "thresholdless lasing" and a maximum intracavity photon number which is rate-limited due to the (irreversible) recycling of the one atom through its energy levels. Additionally, the one-atom laser exhibits photon antibunching and sub-Poissonian photon statistics, evidence that it is a manifestly quantum light source. For comparison with our experimental results, we have extensively analyzed the theory of "lasing" in the strong-coupling regime [34].

The single-atom laser produces a nonclassical stream of photons, but we can also use our atom-cavity system to generate single photons on demand [2]. Here we apply the fields Ω_3 and Ω_4 as a sequence of pulses. In conjunction with the strong coupling g, Ω_3 performs a "dark-state" transfer of an atom between hyperfine ground states $F = 3 \rightarrow 4$ [35]. Simultaneously, it creates a photon in the intracavity field which subsequently exits the cavity with a transverse spatial profile fixed by the TEM_{00} mode of the cavity (i.e., as a Gaussian beam) and with a temporal profile determined by the time-dependence of the Ω_3 field, which is under external control. After a brief period with no external illumination, an Ω_4 pulse is then used to recycle the atom to the $F = 3$ ground state as a source for subsequent photons. Strong coupling between the $F' = 3$ and $F = 4$ manifolds means that each cycle generates an intracavity photon with efficiency approaching 100%, with an overall efficiency of $(69 \pm 10)\%$ for creating an unpolarized photon in the cavity output. Due to our extended trapping times, each atom generates about 1.4×10^4 single photons before it is heated out of the FORT. The cavity output is directed to two photoelectric detectors at the ports of a beam splitter, leading to an overall detection efficiency of $\sim 2.4\%$ (intracavity photon to photoelectric event). A large suppression of two-photon events is measured by way of correlation functions for photoelectric events from the two detectors, with the largest observed suppression being a factor $R \geq 150$ relative to a coherent state. We thereby demonstrate the predominantly single-photon character of our source. The remaining two-photon character is created principally by "contamination" from rare events in which two atoms are simultaneously loaded into the trap.

Such two-atom events raise the important question of whether it is possible to prepare a chosen number of atoms within a cavity. Our method of atom collection – releasing a cold cloud of $\sim 10^5$ atoms above our cavity – relies on the prohibitive geometry of the narrow cavity opening to admit only a few atoms at a time. If we limit the number of atoms in the cloud or the efficiency of the cooling beams, we can reduce the probability of loading more than one atom but can never eliminate it completely. However, if instead we load several atoms at once into the cavity, we have found that by monitoring the cavity transmission with a probe beam, we can watch the atoms "boil off" one by one from the trap [3]. The signature of these departures is a series of step-like plateaus in the cavity transmission, such that the decay of atom number $N \gg 3 \rightarrow 2 \rightarrow 1 \rightarrow 0$ is easily discernible in real time. An analysis of the single photon generation data shows that at long trapping times (when it is much less likely to have two atoms still in the cavity), the suppression of two-photon events is much improved. In future work, monitoring probe transmission levels could be an efficient means of loading exactly one atom into a cavity, or selecting the number of atoms to be entangled via quantum information

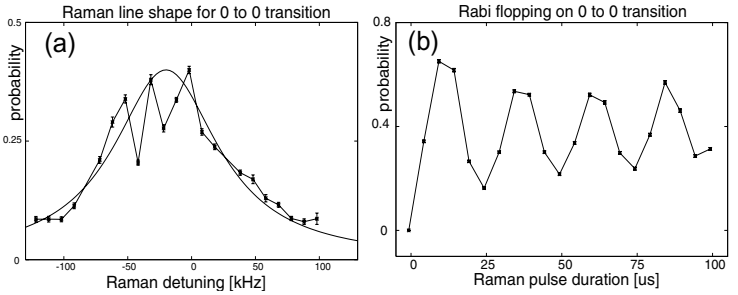

FIGURE 2. Raman transitions for one atom trapped in a cavity: (a) frequency shift of the Raman resonance, and (b) "Rabi flopping" oscillations between Cesium ground states. We drive the transition $(F = 3, m_F = 0) \leftrightarrow (F = 4, m_F = 0)$ with $\Omega_E \sim 50$ kHz for a pulse of duration $\Delta t = 100\mu$s. In (a), a Raman detuning $\delta = 0$ corresponds to the known Cesium hyperfine splitting. We scan the Raman laser frequency around this point and plot the probability that the atom has been transferred to the $F = 4$ ground state; note the red-shifted line shape peak due to small differences in FORT shifts for the $F = 3, 4$ levels. In (b), we apply Raman pulses with varying durations up to 100 μs. After each pulse, the atom is queried with a probe laser to determine whether it is in the $F = 4$ ground state.

protocols (e.g., as in Ref. [36]).

NEW TOOLS FOR CAVITY QED

What do we still hope to add to our cavity QED toolbox? Without interfering with atom-cavity interactions, we need to be able to characterize the atom's environment while it is trapped within the FORT. Specifically, we would like to know the magnetic field that the atom experiences, the initial value and any temporal variation of the energy at which it is trapped, and the properties of the FORT surrounding it (for example, the intracavity polarization). Furthermore, we hope to improve our control of the atom's center-of-mass motion within the cavity, ultimately cooling to the ground state. Currently, we employ blue-detuned Sisyphus cooling for motion transverse to the cavity axis, but we would also need to implement an axial cooling scheme. Finally, we aspire to achieve coherent control of the atomic internal states. The long-term goal of realizing quantum networks within the cavity QED setting relies upon the ability to generate, process, and store information in cavities which act as quantum nodes [37, 38]; creating coherent superpositions of hyperfine states would be an important step in this direction.

One powerful technique – Raman transitions between hyperfine ground states – has the potential to address all three goals of characterization, external cooling, and internal control. In order to implement Raman transitions within the constraints of our cavity geometry, we have developed a new technique that employs the intracavity FORT field itself together with a superimposed beam from a second 936 nm laser, likewise mode-matched to the cavity and phase-locked to the original FORT beam. Both lasers drive the same cavity mode, but while the FORT beam (Rabi frequency Ω_F) is resonant with the cavity, the new Raman beam (Rabi frequency Ω_R) is detuned by the Cesium ground state hyperfine splitting plus an additional shift δ. If Δ is the approximate detuning

of the laser frequencies for Ω_F, Ω_R from the atomic resonance, then in the limit that $\Delta \gg \Omega_F, \Omega_R, \delta, \gamma$, the effective Rabi frequency for transitions between hyperfine states is given by $\Omega_E(t) = \frac{\Omega_F \Omega_R(t)}{2\Delta}$.

Fig. 2 presents the initial evidence that we are able to drive Raman transitions of a Cesium atom in a cavity. After an atom is cooled into the FORT, it is prepared by optical pumping in the $F = 3, m_F = 0$ ground state. We apply a magnetic field along the cavity axis in order to create known frequency splittings (on the order of a few Megahertz) between the Zeeman levels, and thereby focus on only one Zeeman transition. Subsequently, the Raman laser is switched on in order to drive the $(F = 3, m_F = 0) \leftrightarrow (F = 4, m_F = 0)$ transition with Rabi frequency $\Omega_E = 50$ kHz for duration 100μs. For the data shown in (a), the Raman laser frequency is detuned over a range of hundreds of kilohertz in the vicinity of the hyperfine splitting; after exposure to Raman light at a given frequency, a probe pulse along the cavity axis resonant with the $F = 4 \rightarrow F = 5'$ Cesium transition at 852 nm measures whether the atom is in the $F = 4$ ground state, with the probability for a transition plotted as the ordinate in Fig. 2. The result is a Raman line shape whose width is given by the experimentally determined Rabi frequency $\Omega_E(t)$ and whose peak is shifted 20 kHz to the red of the hyperfine splitting, corresponding to a relative shift of the $F = 3$ and $F = 4$ levels due to the FORT potential that can be calculated; a sketch of the calculation is as follows:

$$U_4 - U_3 \sim \frac{I_F}{\Delta} - \frac{I_F}{\Delta + \delta_A} \sim \frac{\delta_A}{\Delta} U_4 \sim (2\pi)(20kHz) \tag{5}$$

Here U_4 and U_3 are the potential well depths of the FORT in the $F = 4$ and $F = 3$ ground states, respectively, and δ_A is the hyperfine splitting. The agreement of observed and calculated lineshapes (e.g., the width and shift in the peak) indicates that we can perform Raman spectroscopy with an accuracy on the order of tens of kHz. Meanwhile, in (b), the Raman beam is pulsed for various short time intervals. A probe pulse subsequently queries the atom to determine its ground state, and the resulting probabilities as a function of pulse duration display the familiar oscillations of "Rabi flopping."

Having demonstrated Raman transitions within our cavity, we turn to the techniques of Raman sideband cooling, already well-established for trapped ions [see the contributions by the groups of D. Wineland and R. Blatt in this volume] and for alkali atoms in free space [e.g., see Refs. [39, 40]]. If n denotes the vibrational state of the atom in the FORT potential, then slightly higher frequencies can drive the atom from $(F = 3, m_F = 0, n)$ to $(F = 4, m_F = 0, n+2)$, while lower frequencies can drive the atom to $(F = 4, m_F = 0, n-2)$. Note that because the FORT laser and Raman laser are spatially overlapped, symmetry arguments only permit even Δn transitions. Thus a Raman scan (Fig. 3) displays three peaks: blue and red sideband peaks, corresponding to transitions to higher and lower vibrational states, respectively, surrounding a central carrier. The positions of these peaks correspond reasonably well to the expectation $\pm 2\nu_0 \simeq \pm 1.1$ MHz, where ν_0 is the vibrational frequency for harmonic motion at the antinode of the FORT, which is independently determined from the FORT and Cs parameters. However, we do not yet understand the observed lineshapes or the loss of contrast evidenced in Fig. 3. Preliminary attempts at cooling center-of-mass motion via Raman sidebands suggest that we can extend the lifetime of trapped atoms within our cavity. When cooling, we

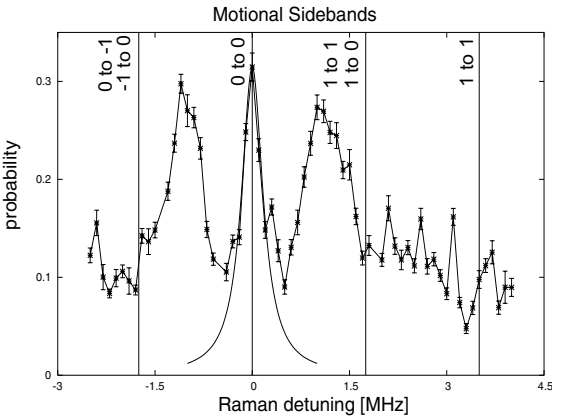

FIGURE 3. Motional Raman sidebands for one trapped atom. The atom is initially prepared as described in Fig. 2 and in the text. We drive the transition $(F = 3, m_F = 0) \leftrightarrow (F = 4, m_F = 0)$ with $\Omega_E =$ 200 kHz for various Raman detunings δ. The detuning $\delta = 0$ is chosen to coincide with the transition between $m_F = 0$ levels; the frequencies of other (suppressed) transitions between Zeeman levels are indicated.

omit the axial magnetic bias field so that all Zeeman levels will now have access to the Raman light.

Using Raman transitions, we are thus able to rotate a Cesium atom between its internal ground states, and we hope to cool atoms along the cavity axis close to the vibrational ground states. Additionally, Raman scans can provide diagnostic information about the magnetic fields experienced by an intracavity atom. For this technique, we again omit a bias field and optically pump the atom so as to randomly distribute it among all possible Zeeman levels within one of the $F = 3, 4$ manifolds. Then scans such as Fig. 3 will reveal transitions for $\Delta m_F = \pm 1$ ($\Delta m_F = 0$) in the presence of transverse (axial) fields, while the frequency spacing between transitions will indicate field strength. As a final step, we can adjust field strengths of external magnetic bias coils in order to create a desired intracavity field.

Finally, we have made initial efforts at measuring the temperature of trapped atoms via adiabatic reduction of trap depth [41]. The protocol for this measurement requires loading an atom into a trap with depth U_0, then adiabatically ramping down the trap depth to a second level U_1, ramping the trap depth back up to its initial level, and at last using a probe measurement to see if the atom has survived this process. We repeat the protocol for various depths U_1 and plot survival probability as a function of this minimum depth. Using the methods of [41], we convert well depths to initial atom energies. A fit of our data to the Boltzmann distribution gives a value of $k_B T = 0.5mK$, or $0.3U_0$. We hope to use this method to evaluate our progress in Raman sideband cooling.

Having traced the path of strong coupling through to the present, it is tempting to speculate upon where the future will lead us. Perhaps the answer lies with atoms coupled not to optical Fabry-Perot cavities but instead to the evanescent fields of solid-state toroid microcavities. Recent progress in this field [42] has produced structures

with quality factors $Q \sim 4 \times 10^8$ and which may be reduced in size to give $g_0 \sim 400$ MHz. The critical atom and photon numbers for such a system with atomic Cs would be, respectively, $N_0 \sim 5 \times 10^{-7}$ and $m_0 \sim 3 \times 10^{-5}$ [43]. Another promising avenue is provided by atoms coupled to the evanescent fields of photonic bandgap cavities [44]. With regard to these devices, recent theoretical work [45] points out that new issues arise when the coherent coupling g is greater than the hyperfine level splitting, forcing us to look beyond conventional models of the atom-field interaction as we push further into the strong coupling regime.

ACKNOWLEDGMENTS

This work was supported by the National Science Foundation (NSF), by the Caltech MURI Center for Quantum Networks, by the Advanced Research and Development Activity (ARDA), and by the Office of Naval Research (ONR).

REFERENCES

1. J. McKeever, A. Boca, A. D. Boozer, J. R. Buck, and H. J. Kimble, Nature **425**, 268 (2003); for commentary, see H. Carmichael and L. A. Orozco, Nature **425**, 246 (2003).
2. J. McKeever, A. Boca, A. D. Boozer, R. Miller, J. R. Buck, A. Kuzmich, and H. J. Kimble, Science **303**, 1992 (2004).
3. J. McKeever, J. R. Buck, A. D. Boozer, and H. J. Kimble, Phys. Rev. Lett. (to be published, 2004).
4. E. M. Purcell, Phys. Rev. **69**, 681 (1946).
5. D. Kleppner, Phys. Rev. Lett. **47**, 233 (1981).
6. For a review, see E. A. Hinds, Adv. At. Mol. Phys. **28**, 237 (1991).
7. H. B. G. Casimir and D. Polder, Phys. Rev. **73**, 360 (1948).
8. D. Meschede, W. Jhe, and E. A. Hinds, Phys. Rev. A **41**, 1587 (1990).
9. For early reviews of the field, see P. Berman, ed., *Cavity Quantum Electrodynamics*, Academic Press, San Diego (1994); S. Haroche and D. Kleppner, Physics Today **42**, 24 (1989).
10. G. Gabrielse and H. Dehmelt, Phys. Rev. Lett. **55**, 67 (1985).
11. R. S. Van Dyck, Jr., P. B. Schwinberg, and H. G. Dehmelt, in *Atomic Physics 9*, World Scientific, Singapore (1984).
12. L. Brown and G. Gabrielse, Rev. Mod. Phys. **58**, 233 (1986).
13. E. T. Jaynes and F. W. Cummings, Proc. IEEE **51** 89 (1963).
14. H. J. Kimble, Phys. Scr. **T76**, 127 (1998).
15. An excellent scientific tutorial of cavity QED in the microwave domain is given by P. Meystre in Progress in Optics, Vol. XXX, ed. E. Wolf (Elsevier Science Publishers B.V., Amsterdam, 1992), p. 261.
16. H. Mabuchi, Q. A. Turchette, M. S. Chapman, and H. J. Kimble, Opt. Lett. **21**, 1393 (1996).
17. G. Rempe, R. J. Thompson, R. J. Brecha, W. D. Lee, and H. J. Kimble, Phys. Rev. Let. **67**, 1727 (1991).
18. R. J. Thompson, G. Rempe, and H. J. Kimble, Phys. Rev. Lett. **68**, 1132 (1992).
19. P. Maunz, T. Puppe, I. Schuster, N. Syassen, P. W. H. Pinske, and G. Rempe, Nature **428**, 50 (2004).
20. Y. Shimizu, N. Shiokawa, N. Yamamoto, M. Kozuma, T. Kuga, L. Deng, and E. W. Hagley, Phys. Rev. Lett. **89**, 233001 (2002).
21. L. V. Hau, S. E. Harris, Z. Dutton, and C. H. Behroozi, Nature **397**, 594 (1999).
22. S. Kuhr, W. Alt, D. Schrader, M. Müller, V. Gomer, and D. Meschede, Science **293**, 278 (2001).
23. J. A. Sauer, K. M. Fortier, M. S. Chang, C. D. Hamley, and M. S. Chapman, Phys. Rev. A **69**, 051804 (2004).
24. G. R. Guthörlein, M. Keller, K. Hayasaka, W. Lange, and H. Walther, Nature **414**, 49 (2001).
25. M. Keller, B. Lange, K. Hayasaka, W. Lange, and H. Walther, Nature (to be published, 2004).

26. A. B. Mundt, A. Kreuter, C. Becher, D. Leibfried, J. Eschner, F. Schmidt-Kaler, and R. Blatt, Phys. Rev. Lett. **89**, 103001 (2002).
27. C. J. Hood, T. W. Lynn, A. C. Doherty, A. S. Parkins, and H. J. Kimble, Science **287**, 1447 (2000).
28. A. C. Doherty, T. W. Lynn, C. J. Hood, and H. J. Kimble, Phys. Rev. A. **63**, 013401 (2000).
29. J. Ye, D. W. Vernooy, and H. J. Kimble, Phys. Rev. Lett. **83**, 4987 (1999).
30. H. J. Kimble, C. J. Hood, T. W. Lynn, H. Mabuchi, D. W. Vernooy, and J. Ye, in *Laser Spectroscopy: XIV International Conference*, (R. Blatt, J. Eschner, D. Leibfried, F. Schmidt-Kaler, eds.) World Scientific, Singapore (1999), 80.
31. H. Katori, T. Ido, and M. Kuwata-Gonokami, J. Phys. Soc. Jpn. **68**, 2479 (1999); T. Ido, Y. Isoya, and H. Katori, Phys. Rev. A **61**, 061403 (2000).
32. S. J. van Enk, J. McKeever, H. J. Kimble, and J. Ye, Phys. Rev. A **64**, 013407 (2001).
33. J. McKeever, J. R. Buck, A. D. Boozer, A. Kuzmich, H.-C. Nägerl, D. M. Stamper-Kurn, and H. J. Kimble, Phys. Rev. Lett. **90**, 133602 (2003).
34. A. D. Boozer, A. Boca, J. R. Buck, J. McKeever, and H. J. Kimble, Phys. Rev. A **70**, 023814 (2004).
35. Adiabatic transfer via dark eigenstates is described for classical fields by J. R. Kuklinski, U. Gaubatz, F. T. Hioe, and K. Bergmann, Phys. Rev. A. **40**, 6741 (1989), and for quantum fields by A. S. Parkins, P. Marte, P. Zoller, and H. J. Kimble, Phys. Rev. Lett. **71**, 3095 (1993).
36. L.-M. Duan and H. J. Kimble, Phys. Rev. Lett. 90, 253601 (2003).
37. J. Cirac, P. Zoller, H. J. Kimble, and H. Mabuchi, Phys. Rev. Lett. **78**, 3221 (1997).
38. H.-J. Briegel, S. J. van Enk, J. I. Cirac, P. Zoller, *The Physics of Quantum Information*, (D. Bouwmeester, A. Ekert, A. Zeilinger, eds.) Springer, Berlin (2000), ch. 6, 8.
39. S. E. Hamann, D. L. Haycock, G. Klose, P. H. Pax, I. H. Deutsch, and P. S. Jessen, Phys. Rev. Lett. **80**, 4149 (1998)
40. V. Vuletić, C. Chin, A. J. Kerman, and S. Chu, Phys. Rev. Lett. **81**, 5768 (1998).
41. W. Alt, D. Schrader, S. Kuhr, M. Müller, V. Gomer, and D. Meschede, Phys. Rev. A **67**, 033403 (2003).
42. K. Vahala, Nature **424**, 839 (2003).
43. S. M. Spillane, T. J. Kippenberg, K. J. Vahala, K. W. Goh, E. Wilcut, H. J. Kimble, Phys. Rev. A (submitted, 2004).
44. J. Vuckovic, M. Loncar, H. Mabuchi, and A. Scherer, Phys. Rev. E 65, 016608 (2002).
45. A. S. Parkins and K. Birnbaum, in preparation.